Beryllium–Cyclobutadiene Multidecker Inverse Sandwiches: Electronic Structure and Second-Hyperpolarizability

ARTICLE *in* THE JOURNAL OF PHYSICAL CHEMISTRY A · OCTOBER 2013

Impact Factor: 2.69 · DOI: 10.1021/jp407563f · Source: PubMed

2 AUTHORS:

Kaushik Hatua
Indian Institute of Engineering Science and Te…
13 PUBLICATIONS **48** CITATIONS
SEE PROFILE

Prasanta Nandi
Indian Institute of Engineering Science and Te…
17 PUBLICATIONS **102** CITATIONS
SEE PROFILE

THE JOURNAL OF PHYSICAL CHEMISTRY A

Article

pubs.acs.org/JPCA

Beryllium-Cyclobutadiene Multidecker Inverse Sandwiches: Electronic Structure and Second-Hyperpolarizability

Kaushik Hatua and Prasanta K. Nandi*

Department of Chemistry, Bengal Engineering and Science University, Shibpur, Howrah 711 103, India

Supporting Information

ABSTRACT: Beryllium forms stable sandwich and inverse sandwich complexes with the cyclobutadiene molecule. Two types of multidecker complexes are designed. Multidecker inverse sandwiches are found to be thermally more stable than the corresponding sandwich complexes. The average distance between two consecutive metals and the two consecutive cyclobutadiene rings increase gradually on increasing size of the chosen inverse sandwich complexes. The density functional theory functionals B3LYP, BHHLYP, BLYP, M06, CAM-B3LYP, and B2PLYP in conjunction with the 6-311++G (d, p) basis set have been employed for calculating the third-order electric response properties of the chosen beryllium-cyclobutadiene complexes and the results obtained for each functional are found to have a consistent trend. Compared to the normal sandwich compounds the second-hyperpolarizability of inverse sandwiches is predicated to be larger, which fairly correlates with the extent of ground-state polarization. The significant enhancement of cubic polarizability of higher-order multidecker inverse sandwiches arises from the strong coupling between the ground and the low lying charge transfer excited states. The rather strong enhancement of second-hyperpolarizability on increasing size of the beryllium-multidecker inverse sandwiches may provide a new route to design efficient nonlinear optical materials.

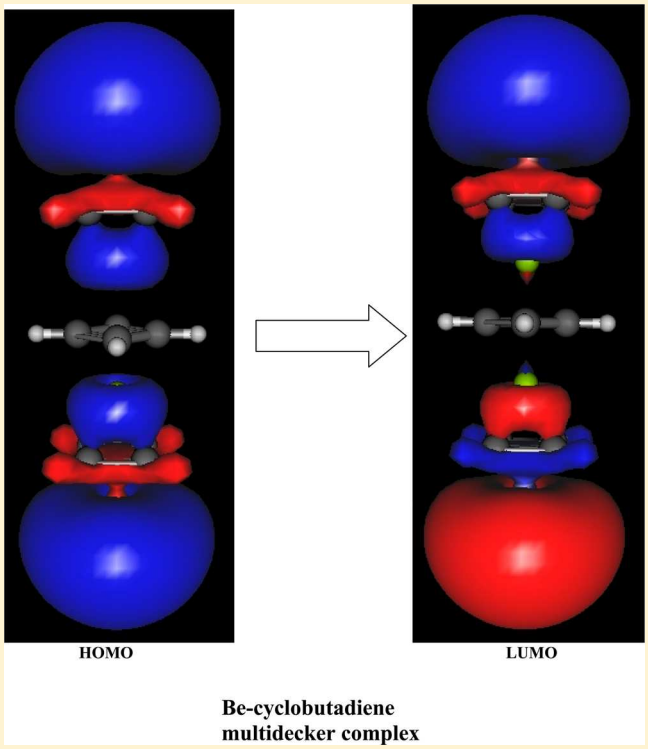

I. INTRODUCTION

Demand of potential nonlinear optical (NLO) active materials in photonic devices, optical data storage, data processing, and data transmission has been grown enormously in recent years, and theoretical research in conjunction with experiment made significant contributions in this progress.[1−3] Study of NLO properties has been diversified in different dimension in this era. Early investigations of NLO properties of donor−acceptor-substituted π-conjugative charge transfer molecules[1−8] have now been renewed in the light of modern approach of enhancement of optical responses. Nakano et al. showed that compounds having intermediate diradical character would possess appreciably larger cubic polarizability compared to that of pure singlet or triplet states.[9−11] Robust calculations of hyperpolarizability of atomic rare gases[12] and rare gas inserted fluorides[13−15] recently have been carried out. The electride systems, doped by alkali metal, can induce large first-hyperpolarizability in conjugated organic chains or molecules.[16−21] Alkali metal doping can also enhance second-hyperpolarizability.[22] The origin of large hyperpolarizabilities of radical ion pair salts $M_2^{\bullet+}TCNQ^{\bullet-}$ (M = Li, Na, K) has been ascribed to the excess electron transition from the metal.[23] Pendent atom in polymer backbone remarkably enhances first-hyperpolarizability.[24] Fullerene-based sandwich-like superrmolecules[25] CpLi-C_{60} possess large NLO properties. Multilithium salt of tubiform [n] cyclane has been considered to optimize the first-hyperpolarizability.[26] The excess electron concept has also been exploited in boron nitride nanotube[27] to produce significantly large first-hyperpolarizability.

Be-based organometallic complexes are found to be the promising NLO active materials[28] due to their weak linear optical transition. Since metallocenes (Cp-M-Cp, Cp = cyclopentadienyl ligand) have very interesting bonding and structural characteristics it has been becoming an active area of research in the recent years.[29,30] Crystallographic information of lithocene (LiCp), sodacene (NaCp), and KCp are well-known[31] and solid-

Received: July 30, 2013
Revised: October 24, 2013
Published: October 28, 2013

Scheme 1. Beryllium-Cyclobutadiene Complexes

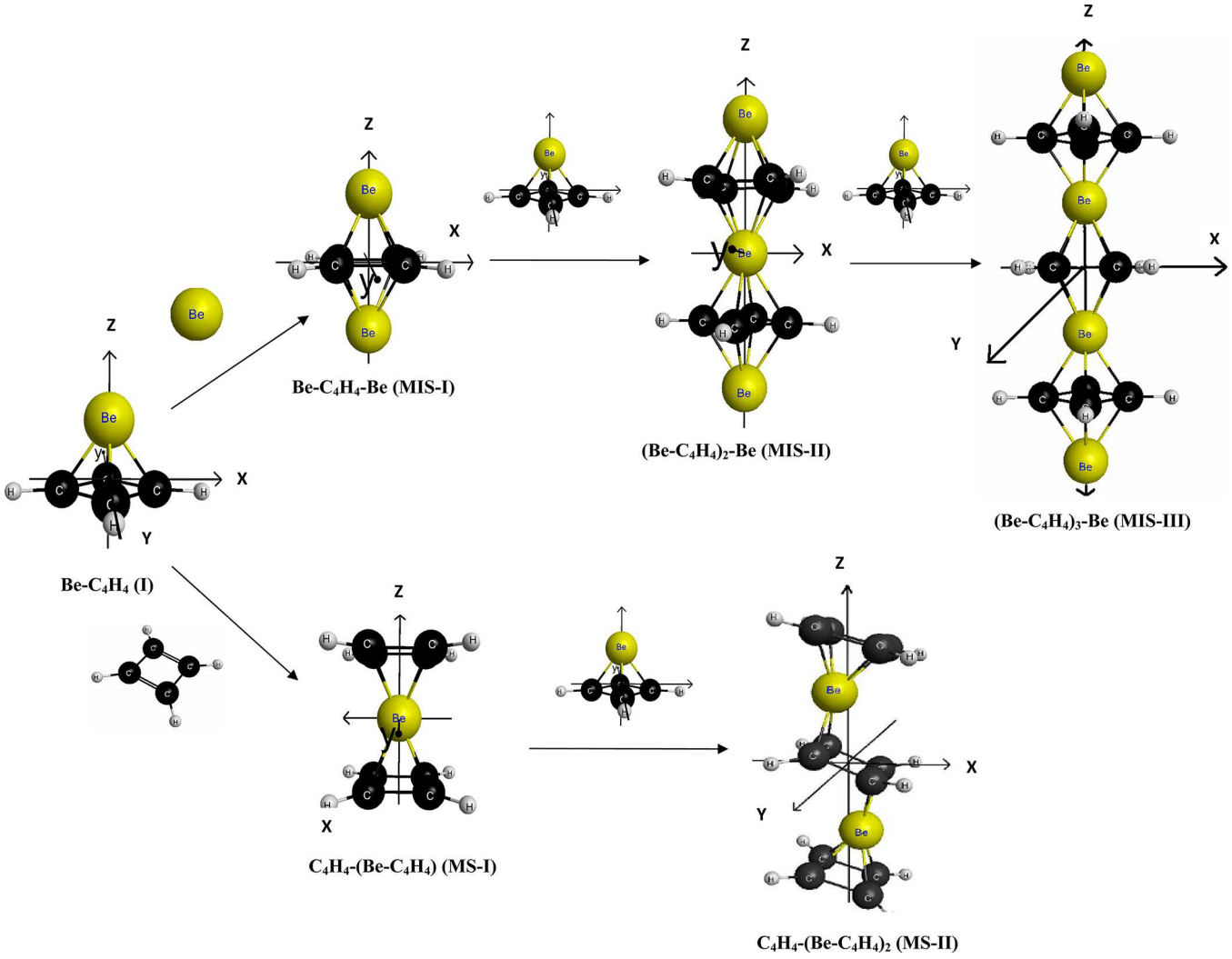

state NMR studies revealed the nature of electronic environment around the metal−ligand complexes.[32,33] Extensive quantum chemical investigations of main group metallocenes are known.[34] Theoretical investigation of multimetallocenes (CpM_nCp) of Be, Mg, Ca revealed[35] that Cp-M_n-Cp species with $n > 2$ are thermodynamically unstable with respect to loss of one metal atom except for Be. While the metal−metal interaction is purely covalent in dimetallocenes,[36,37] metal−ligand interaction is ionic in nature.[38] However, such sandwich complexes of cyclobutadiene (C_4H_4) are unfamiliar unless a recent study of the complex of the type $[Cp\text{-}Ga\text{-}Cp]^+$, which is a stable isolated salt,[39] inspires the theoretical work on structural and thermal properties of the type of complex [E-C_4H_4-E] of group 13 metals[40,41] in different oxidation states. This kind of complex is named as inverse sandwich complex. Although a lot of structural information about these complexes is available in the literature, nothing is known about their electric response property.

In the present work, we have considered a number of multidecker complexes of Be with cyclobutadiene molecule (C_4H_4) based on the Be-half-sandwich complex Be-C_4H_4 (**1**). Starting from this complex, one can add to it either a C_4H_4 unit or a Be atom to obtain either a normal sandwich complex [C_4H_4-Be-C_4H_4] (**MS-I**) or an inverse sandwich complex [Be-C_4H_4-Be] (**MIS-I**) as shown in Scheme 1. These two complexes would be the starting material for synthesis of Be-cyclobutadiene sandwich (**MS-II**) and inverse sandwich (**MIS-II**) complexes. The [C_4H_4-Be-C_4H_4] complex is known as multidecker sandwich of first-order (**MS-I**) while [Be-C_4H_4-Be] complex is called a multidecker inverse sandwich complex of first-order (**MIS-I**). Then further addition of a Be-C_4H_4 unit to **MS-I** and **MIS-I** results in the formation of second-order sandwiches. In the present investigation, we have considered multidecker sandwich up to the second order (**MS-II**) and multidecker inverse sandwich up to the third-order (**MIS-III**) each of which consists of three C_4H_4 units. The general formula of **MIS** of "*n*th" order can be expressed as Be-$(C_4H_4\text{-}Be)_n$ for $n \neq 0$.

II. COMPUTATIONAL METHODS

Geometry optimizations have been carried out by employing the widely used B3LYP and MP2 methods for the sake of comparison. The split valence triple-ζ quality basis set augmented with diffuse functions and "d" and "p" type polarization functions, that is, 6-311++G(d,p) basis set has been used for all calculations. The stabilities of the structures (Scheme 1) on the potential energy surface have been checked by calculating harmonic vibrational frequencies at the same level which are found to be real. The MP2 optimized geometry has been taken in the subsequent calculation of nonlinear optical

dx.doi.org/10.1021/jp407563f | J. Phys. Chem. A 2013, 117, 12581−12589

Table 1. MP2 and B3LYP[a] Optimized CC Bond Lengths (Å), the Shortest Be−(C_4H_4) Distance and the MP2 Calculated Natural Atomic Charges (au), Dissociation Energy (ΔE_D, kcal/mol)[b] and Stabilization Energy ($-\Delta E_S$, kcal/mol) of Be-Complexes (Scheme 1) Obtained for the 6-311++G(d,p) Basis Set

					Q		
complex	CC	Be−(C_4H_4)[c]	ΔE_D	ΔE_S	C	Be	H
C_4H_4 (C_{2v})	1.444				−0.340		0.198
	1.435						
C_4H_4 (D_{2h})	1.349, 1.572				−0.192		0.192
	1.333, 1.576						
I (C_{4v})	1.480	1.384	56.9	56.9	−0.439	0.850	0.226
	1.473	*1.375*					
MS-I (D_{2h})	1.406, 1.534	1.575	119.8	60.3	−0.275	0.385	0.226
eclipsed rings	*1.390, 1.533*	*1.600*					
MIS-I (D_{4h})	1.491	1.537	115.8	56.2	−0.484	0.450	0.258
	1.489	*1.508*					
MS-II (D_{1d})	(1.453, 1.511)[d], (1.428, 1.513)[e]	1.674[d], 1.483[e]	246.4	63.2	−0.296[d], −0.298[e]	0.413	0.230[d], 0.228[e]
eclipsed rings	*(1.427, 1.515)[d], (1.417, 1.508)[e]*	*1.709[d], 1.487[e]*					
MIS-II (S_8)	1.483	1.614[d], 1.553[e]	255.0	79.6	−0.451	0.689[d]	0.255
staggererd rings	*1.464*	*1.632[d], 1.481[e]*				0.311[e]	
MIS-III (D_{4h})	1.485[d], 1.480[e]	(1.625,1.626)[d], 1.601[e]	409.9	95.3	−0.450[d]	0.876[d]	0.249[d],
staggererd rings	*1.479[d], 1.479[e]*	*(1.586,1.663)[d], 1.480[e]*			−0.484[e]	0.451[e]	0.255[e]

[a]B3LYP bond lengths are in italic. [b]The energy quantities are calculated with respect to the lower energy D_{2h} structure of C_4H_4 molecule. [c]The Be−(C_4H_4) distance refers to the shortest distance between the metal and the nearest cyclobutadiene ring. [d]Middle Be−(C_4H_4) distance. [e]End Be−(C_4H_4) distance.

properties. Binding energy of the Be-complexes in the isolated gas phase has been calculated as the energy difference, $\Delta E_D = nE_{C4H4} + mE_{Be} - E_{Complex}$ (n = 1−3 and m = 1−4). Besides this, the energy difference, $\Delta E_S = E_{products} - E_{reactants}$ has also been calculated for each of the following reactions 1−6 to find the relative stability or ease of formation of the higher-order complex with respect to the lower-order complex. The energy differences ΔE_D and ΔE_S are calculated with respect to the lower-energy rectangular structure of cyclobutadiene.

$$C_4H_4 + Be \rightarrow Be\text{-}C_4H_4\ (\mathbf{I}) \quad (1)$$

$$C_4H_4 + Be\text{-}C_4H_4\ (\mathbf{I}) \rightarrow C_4H_4\text{-}(Be\text{-}C_4H_4)\ (\mathbf{MS\text{-}I}) \quad (2)$$

$$Be\text{-}C_4H_4\ (\mathbf{I}) + Be \rightarrow (Be\text{-}C_4H_4)\text{-}Be\ (\mathbf{MIS\text{-}I}) \quad (3)$$

$$C_4H_4\text{-}Be\ (\mathbf{I}) + C_4H_4\text{-}(Be\text{-}C_4H_4)\ (\mathbf{MS\text{-}I}) \rightarrow C_4H_4\text{-}(Be\text{-}C_4H_4)_2\ (\mathbf{MS\text{-}II}) \quad (4)$$

$$Be\text{-}C_4H_4\ (\mathbf{I}) + (Be\text{-}C_4H_4)\text{-}Be\ (\mathbf{MIS\text{-}I}) \rightarrow (Be\text{-}C_4H_4)_2\text{-}Be\ (\mathbf{MIS\text{-}II}) \quad (5)$$

$$\mathbf{2}(Be\text{-}C_4H_4)\ (\mathbf{I}) + (Be\text{-}C_4H_4)\text{-}Be\ (\mathbf{MIS\text{-}I}) \rightarrow (Be\text{-}C_4H_4)_3\text{-}Be\ (\mathbf{MIS\text{-}III}) \quad (6)$$

The energy quantities and natural atomic charges are calculated at the MP2/6-311++G(d,p) level.

The mean polarizability ($\langle\alpha\rangle$) is calculated as one-third of the trace of linear polarizability tensor

$$\langle\alpha\rangle = \frac{(a_{xx} + a_{yy} + a_{zz})}{3} \quad (7)$$

The orientationally averaged second-hyperpolarizability ($\langle\gamma\rangle$) has been calculated[1] by using the following expression.

$$\langle\gamma\rangle = \frac{1}{5}[\gamma_{xxxx} + \gamma_{yyyy} + \gamma_{zzzz} + 2(\gamma_{xxyy} + \gamma_{xxzz} + \gamma_{yyzz})] \quad (8)$$

The predominant charge transfer interaction of the chosen complexes takes place along the molecular z-axis (see Scheme 1) and the axial z-component of γ (γ_{zzzz}) has been found to be the major component. The components of polarizability and second-hyperpolarizability are calculated analytically by employing various density functional theory (DFT) functionals BLYP, B3LYP, BHHLYP, CAM-B3LYP, M06, and B2PLYP. It has been well-known that the magnitude of hyperpolarizabilities depends on the choice of DFT functionals employed. Because of the lack of experimental data of second-hyperpolarizability for the investigated complexes, a comparison of the theoretical results obtained by different DFT methods may provide the reliability of present calculations. The pure generalized gradient approximation (GGA) functional BLYP (Becke exchange (B)[42] and Lee−Yang−Parr (LYP) correlation)),[43] hybrid GGA functionals B3LYP (Becke + Slater + 20% HF exchange and LYP + VWNS correlations),[44] BHHLYP (50% HF + 50% Becke88 + 50% LSDA exchange and LYP correlation),[45] and long-range corrected Coulombic-attenuating CAM-B3LYP[46] functionals are the widely used DFT methods for calculation of hyperpolarizabilities. Besides two other DFT methods, B2PLYP (hybrid density functional with perturbative second-order correlation)[47] and M06[48] are also employed in the present study as test cases. Among these, the CAM-B3LYP functional has been found[49,50] to be the more appropriate method for (hyper)polarizability calculations which can reproduce the results obtained with correlated ab initio levels.

All calculations are performed with Gaussian 09 quantum chemical package.[45]

III. RESULTS AND DISCUSSION

3.1. Equilibrium Geometry and Energetics of Be-Cyclobutadiene Complexes. The MP2 and B3LYP optimized

dx.doi.org/10.1021/jp407563f | J. Phys. Chem. A 2013, 117, 12581−12589

Table 2. Basis Set[a] Dependence of Longitudinal Component of Second-Hyperpolarizability (γ_{zzzz}, 10^4 au) Obtained at the B3LYP Level

complex	6-31G (d,p)	6-31++ G (d,p)	6-311G (d,p)	6-311++ G (d,p)	cc-pvdz	cc-pvtz	aug-cc-pvdz	aug-cc-pvtz
I	0.393	3.765	1.102	4.003	8.691	1.597	3.744	4.422
MIS-I	1.404	149.829	6.483	117.951	1.189	13.887	107.157	114.795
MIS-II	2.194	601.808	24.309	516.338	9.889	44.833	523.051	531.255

[a]The γ_{zzzz} values (in 10^4 au) obtained for molecules **I**, **MIS-I**, and **MIS-II** using the d-aug-cc-pVDZ basis set on C and H and aug-cc-pVTZ basis set on Be are 3.806, 118.761, and 533.200, respectively.

CC bond length, shortest beryllium-cyclobutadiene ring [Be-(C_4H_4)] distance, and the MP2 calculated dissociation energies and stabilization energies of the chosen Be complexes obtained for the 6-311++G(d,p) basis set are reported in Table 1. However, the relative accuracy of the structural data obtained by the two methods cannot be judged due to the lack of relevant experimental or other theoretical results. The cyclobutadiene molecule has two different optimized structures. The lower energy (by about 17.4 kcal/mol) rectangular structure is of D_{2h} symmetry while the other with twisted ring (29.8°) is of C_{2v} symmetry. The later has four CC bonds of equal length. However, in the D_{2h} structure, one CC bond is shorter than that of the C_{2v} structure by about 0.09 Å and the other is longer by about 0.13 Å. It is evident that both the MP2 and DFT methods give consistent results of CC bond lengths, in general. The B3LYP calculated CC bond lengths on an average are smaller than the corresponding MP2 results by 0.01−0.02 Å. The Be-(C_4H_4) distance in complexes **I**, **MS-I**, and **MIS-I** obtained at the two levels remains within 0.01−0.03 Å, which, however, show larger differences of the distance between the terminal Be atom and the ring for complexes **MS-II** (0.04 Å/0.01 Å), **MIS-II** (0.02 Å/0.07 Å), and **MIS-III** (0.001 Å/0.12 Å). However, in the following discussion on structures the MP2 calculated bond distances are used unless otherwise stated. Upon complex formation of C_4H_4 with Be the C═C bond of cyclobutadiene ring in complex **I** elongates by about 0.04 Å with respect to C_{2v} structure or elongates by about 0.13 Å and shortens by about 0.09 Å with respect to D_{2h} structure. This indicates a strong electronic polarization of the ring. The later may arise from the significant amount of charge transfer (0.850 au) from metal to the C_4H_4 ring. The mutual competitive interaction of two C_4H_4 rings with the central Be atom in **MS-I** causes the substantial reduction of metal → ring charge transfer (0.385 au) that is reflected by the larger increase of Be-(C_4H_4) distance and shortening of C═C bond lengths. On the other hand, the interaction between the complex **I** and the Be atom as in the case of the inverse sandwich complex **MIS-I,** both the CC bond lengths and the Be-(C_4H_4) distances elongate (vs **I**) but compared to the sandwich complex **MS-I**, the latter distance is shortened by about 0.04 Å while the CC bond length increases/decreases by about 0.08 Å/0.04 Å. This is consistent with the greater amount of charge transfer from Be to the cyclobutadiene ring in **MIS-I** (Table 1) compared to the sandwich complex **MS-I.** The interaction between complexes **MS-I** and **I** results in the formation of complex **MS-II** in which the greater CT interaction (vs **MS-I**) leads to rather stronger polarization leading to the significant increase of the central Be-(C_4H_4) distance and the C═C bond lengths. The distance (**MP2**/**B3LYP**) between two successive cyclobutadiene rings increases from 3.150 Å/3.157 Å in **MS-I** to 3.200 Å/3.196 Å in **MS-II**.

The interaction of two metal atoms on the terminal C_4H_4 ring or interaction between complexes **I** and **MS-I** along *Z*-axis result in the formation of multidecker inverse sandwich **MIS-II.** The appreciably greater amount of CT from the central Be atom in **MIS-II** (0.689 au vs 0.385 au in **MS-I**) to the C_4H_4 ring results in rather greater elongation of CC bond lengths and the distance of separation between the rings by 3.228 Å/3.264 Å (vs 3.150 Å/3.157 Å in **MS-I**). Likewise, the formation of **MIS-III** arising from the interaction between two metal atoms and the complex **MS-II** or interaction between complexes **I** and **MIS-II** along *Z*-axis is accompanied by the maximum amount of CT from the middle Be atoms (0.876 au). It is interesting to note that the magnitude of charge transfer (0.451 au) from the terminal Be atoms is found to be identical to that in the complex **MIS-I.** The distance between the two consecutive rings in **MIS-III** is now 3.251 Å/3.249 Å.

The calculated dissociation energy (ΔE_D) obtained for the chosen Be-cyclobutadiene complexes has been found to be positive which indicates that the complexes are sufficiently stable. The relative stability increases with increasing size of the complexes in the order: **MS-I** < **MS-II** (by 126 kcal/mol), **MIS-I** < **MIS-II** (by139 kcal/mol), and **MIS-II** < **MIS-III** (by 155 kcal/mol). Thus the cooperative effect on the binding strength is present for the chosen complexes especially in the case of the inverse sandwich complexes. In order to find the energetically favorable approach for growing two kinds of complexes (sandwich and inverse sandwich) with increasing size starting from the complex **I**, the calculated energy quantity ΔE_S associated with the addition reactions 1−6 (in Section II) may be useful. The relative ease of formation of complexes as indicated by the ΔE_S values (Table 1) increases in the order, **I** → **MS-I** → **MS-II** for the sandwich complexes and in the order, **I** → **MIS-I** → **MIS-II** → **MIS-III** for the inverse sandwich complexes. However, in the formation of multidecker inverse sandwiches **MIS-II** and **MIS-III** the calculated ΔE_S values are found to be rather significant which may be attributed to the cooperative bonding interaction. It should be worth mentioned that the average distance (MP2/B3LYP) between two successive metal atoms in the inverse sandwich complexes increases in the order **MIS-I** (3.074 Å/3.018 Å) → **MIS-II** (3.168 Å/3.112 Å) → **MIS-III** (3.235 Å/3.153 Å), which indicates increasing polarizability along the *Z*-axis.

3.2. Static Electronic Polarizability and Second-Hyperpolarizability. Because the charge transfer interaction between the metal and cyclobutadiene ring takes place along the molecular *Z*-axis, the results of longitudinal component of polarizability α_{zz} (**Table S1** of Supporting Information) and second-hyperpolarizability γ_{zzzz} which are the dominant components are reported along with the corresponding mean values in the present work. It should be mentioned that due to the centrosymmetric nature, the chosen complexes have both the ground state dipole moment and first-hyperpolarizability zero. Let us first consider the effect of the size of basis set on the third-order response property. For this purpose three representative complexes **I**, **MIS-I**, and **MIS-II** are chosen for calculating their second-hyperpolarizability by employing a number of basis sets

dx.doi.org/10.1021/jp407563f | J. Phys. Chem. A 2013, 117, 12581−12589

with varying sizes at the B3LYP level of theory. The calculated results are reported in Table 2. It is clear that inclusion of a single set of diffuse functions in the basis set has a dramatic effect on magnitude of second-hyperpolarizability. One of the most important outcome is that the 6-311++G(d,p) basis set of Pople[45] can reproduce the results of second-hyperpolarizability obtained for the Dunning's correlation consistent basis set[51,52] cc-pVTZ augmented (aug-cc-pVTZ) with higher angular momentum diffuse functions. The γ_{zzzz} of **MIS-I** obtained with the 6-311++G(d,p) basis set is overestimated by about 2.7% with respect to the aug-cc-pVTZ basis set. However, for the complex **MIS-II**, γ_{zzzz} obtained at the 6-311++G(d,p) basis set is found to be smaller by about 2.9% when compared to the aug-cc-pVTZ basis set.

In order to find the effect of a second set of diffuse functions on second-hyperpolarizability, the doubly augmented version of Dunning's basis set (d-aug-cc-pVDZ), which includes one additional diffuse function for each angular momentum present in the corresponding aug-cc-pVDZ basis set, has been employed for the representative molecules **I**, **MIS-I**, and **MIS-II**. However, this basis set being not available for Be, the NLO calculations are performed by using the d-aug-cc-pVDZ basis set for C and H atoms, and aug-cc-pVTZ basis set for Be. The combined basis set (d-aug-cc-pVDZ on C and H and aug-cc-pVTZ on Be) compared to the 6-311++G(d,p) basis set changes the γ_{zzzz} value (see footnote of Table 2) by −4.9% for **I**, 0.7% for **MIS-I**, and 3.3% for **MIS-II**. Thus the results of third-order polarizability of the investigated Be-cyclobutadiene complexes obtained using the 6-311++G(d,p) basis set may be considered for qualitative discussions. In view of this, the 6-311++G(d,p) basis set has subsequently been used in the calculation of cubic polarizability.

Because in most of the hyperpolarizability calculations either B3LYP or MP2 optimized geometry is used, we have in the present work considered the MP2 optimized geometries for the computation of second-hyperpolarizability. However, to find the effect of the B3LYP optimized geometry on the second-hyperpolarizability compared to that obtained at the MP2 optimized stuructures, additional calculations of hyperpolarizabilities have also been carried out for some representative complexes at the B3LYP/6-311++G(d,p)//B3LYP/6-311++G(d,p) level and the results are given in Table 3. The magnitudes of

Table 3. Longitudinal Component of Second-Hyperpolarizability (γ_{zzzz}, 10^4 au) and Average Second-Hyper polarizability ($\langle\gamma\rangle$, 10^4 au) Obtained at the B3LYP/6-311++G(d,p) Level Using the B3LYP/6-311++G(d,p) Optimized Geometry

	I	MS-I	MIS-I	MIS-II	MIS-III
γ_{zzzz}	4.013	6.766	123.809	588.858	1535.28
$\langle\gamma\rangle$	4.910	5.037	64.510	236.698	538.797

γ obtained at the B3LYP/6-311++G(d,p) level for the B3LYP and MP2 optimized geometries are found to be significantly different for the higher-order inverse sandwiches **MIS-II** and **MIS-III** which may be attributed to the notable difference of the terminal Be-(C_4H_4) distance at the two levels (see Subsection 3.1). However, the ratio of γ_{zzzz} ($\langle\gamma\rangle$) of the inverse sandwich complexes **MIS-I**, **MIS-II**, and **MIS-III** obtained at the MP2 geometry, 1.0:4.4:10.0 (1.0:3.3:6.5) and at the B3LYP geometry: 1.0:4.8:12.4 (1.0:3.7:8.4) seems to be comparable.

The γ value of sandwich complex **MS-I** being much smaller compared to the inverse sandwich **MIS-I** (Table 4), the second-hyperpolarizability of the next higher-order sandwich complexes **MS-II/III** has not been calculated. Because no experimental or other theoretical results of second-hyperpolarizability are currently available for the studied complexes a comparative discussion of the results obtained by different DFT methods may be useful. It can be noted (Table 4) that for complexes **I** and **MS-I** the results of second-hyperpolarizability obtained by CAM-B3LYP, BHHLYP, M06, and B2PLYP methods vary within a close margin. For the inverse sandwich complex **MIS-I**, the CAM-B3LYP and BHHLYP results of γ_{zzzz} differ only marginally. The B3LYP, BLYP, and M06 results of $\langle\gamma\rangle$ obtained for this complex show a fair agreement while the corresponding BHHLYP and B2PLYP methods compared to the CAM-B3LYP method overestimate $\langle\gamma\rangle$ by 3.4 and 17%, respectively. For complex **MIS-II**, the BLYP and M06 calculated values of γ_{zzzz} are identical although the corresponding $\langle\gamma\rangle$ values differ by about 4%. It can be noted that for the complex **MIS-III**, the γ_{zzzz} and $\langle\gamma\rangle$ values obtained by B3LYP and M06 functionals are rather comparable. However, for **MIS-II** and **MIS-III** complexes the CAM-B3LYP, BHHLYP, and B2PLYP methods predict the magnitude of second-hyperpolarizability at the higher range while the γ values obtained by the remaining DFT functionals remain at the smaller range. Although the results of hyperpolarizability predicted by the chosen DFT functionals differ significantly in some cases, the most general trend of γ obtained for the investigated Be-complexes for a given method is **I** < **MS-I** ≪ **MIS-I** < **MIS-II** ≪ **MIS-III**. The linear polarizability both the longitudinal and mean (Supporting Information) also follow the same order. Hence, the strongest one photon electronic transition should play a significant role in the modulation of the cubic NLO responses of the investigated metal complexes.

In order to interpret the variation of second-hyperpolarizability among the chosen Be-complexes the two-level model[3] of γ corresponding to the most intense (highest oscillator strength) electronic transition has been invoked.

$$\gamma^{2L} \propto \left[\frac{\mu_{gn}^2 \Delta\mu^2}{\Delta E_{gn}^3} - \frac{\mu_{gn}^4}{\Delta E_{gn}^3}\right] \tag{9}$$

The first term containing the dipole moment difference ($\Delta\mu$) between the ground and the predominant charge transfer excited states is the dipolar term. The nondipolar term (second term) depends on the transition dipole moment (μ_{gn}) and the transition energy (ΔE_{gn}). Because the investigated complexes are nondipolar, the second term alone contributes to γ^{2L}.

$$\gamma^{2L} \propto \frac{\mu_{gn}^4}{\Delta E_{gn}^3} \propto \frac{f_{gn}^2}{\Delta E_{gn}^5} \tag{10}$$

In eq 10, f_{gn} (= $(2\Delta E_{gn}\mu_{gn}^2)/3$) is the oscillator strength. The spectroscopic parameters corresponding to the most intense (highest f_{ng}) electronic transition and the two-level contribution of second-hyperpolarizability obtained at the TD-CAM-B3LYP/6-311++G(d,p) level are listed in Table 5. The TD-DFT method using the range separated CAM-B3LYP functional compared to the conventional hybrid functionals can give more accurate results of NLO properties and electronic excitation energies.[53,54] The two-level calculated γ can satisfactorily explain the variation of second-hyperpolarizability.[6] The λ_{max} values show a gradual red-shifting on increasing the size of complexes. The appreciably larger magnitude of γ (by an order of two) of **MIS-I** compared to that of **MS-I** can be accounted for the substantially smaller excitation energy and larger electronic transition moment (Table

dx.doi.org/10.1021/jp407563f | J. Phys. Chem. A 2013, 117, 12581−12589

Table 4. Longitudinal Component of Second-Hyperpolarizability (γ_{zzzz}, 10^4 au) and Average Second-Hyper polarizability ($\langle\gamma\rangle$, 10^4 au) Obtained by Using Different DFT Functionals And the MP2 Optimized Geometry For the 6-311++G (d,p) Basis Set

complex	B3LYP	CAM-B3LYP	BHHLYP	BLYP	M06	B2PLYP
			Second-Hyperpolarizability (γ_{zzzz})			
I	4.003	3.103	3.237	4.758	3.595	3.429
MS-I	7.036	3.129	3.352	10.048	2.953	2.699
MIS-I	117.951	122.763	124.731	119.605	129.006	139.013
MIS-II	516.338	693.615	664.229	463.736	463.469	749.846
MIS-III	1175.40	1766.09	1621.35	1011.97	1159.31	1842.42
			Average Second-Hyperpolarizability ($\langle\gamma\rangle$)			
I	4.942	5.289	3.733	4.654	4.000	3.974
MS-I	5.289	3.569	3.827	7.123	3.607	4.101
MIS-I	60.440	66.401	68.672	60.385	62.534	77.772
MIS-II	202.242	281.311	274.573	180.082	186.961	317.303
MIS-III	393.679	599.732	562.31	337.932	381.357	650.943

Table 5. Excitation Energy (ΔE_{gn}, eV), z-Component of Transition Moment (μ_{gn}, au), Oscillator Strength (f_{gn}, au), Wavelength (λ_{max}, nm), and Two-Level Contribution of Second-Hyperpolarizability (γ^{2L},10^4 au) Corresponding to the Most Intense Electronic Transition ($S_0 \rightarrow S_n$) Obtained at the CAM-B3LYP Level for the 6-311++G(d,p) Basis Set

complex	ΔE_{gn}	μ_{gn}	f_{gn}	λ_{max}	γ^{2L}	$S_0 \rightarrow S_n$	dominant transition configuration
I	5.436	0.922	0.113	228.09	0.004	S_8	HOMO-1→ LUMO+2, HOMO → LUMO +3
MS-I	3.601	2.362	0.492	344.26	0.596	S_2	HOMO −1 → LUMO
MIS-I	1.696	2.804	0.327	730.95	11.368	S_1	HOMO → LUMO
MIS-II	0.879	3.407	0.250	1411.04	177.688	S_1	HOMO → LUMO
MIS-III	0.436	3.339	0.119	2841.49	1340.860	S_2	HOMO → LUMO

5) that is also reflected in their polarizability values (Supporting Information). The complex **MIS-II** can be viewed to be formed from **MS-I** by adding two Be atoms at the terminal sites along the molecular axis in the former or placing complex **I** axially on the top of **MIS-I**. This leads to enhanced charge transfer from the central Be atom compared to the terminal metal atoms (Table 1). This charge redistribution over axial Be atoms in **MIS-II** brings about much stronger polarization of the cyclobutadiene rings with respect to **MS-I** than **MIS-I**. This differential polarization leads to strong enhancement of polarizability and hence second-hyperpolarizability of **MIS-II** when compared to that of **MS-I** instead of **MIS-I**. This is also supported by the substantial changes of transition energy and the transition moment in the transition **MS-I** → **MIS-II** instead of **MIS-I** → **MIS-II**.

The two-level calculated values of second-hyperpolarizability (Table 5) show an increasing parallel trend with the analytically calculated values (Table 4). The two-level model, however, predicts negligibly smaller values of second-hyperpolarizability for molecules **I** and **MS-I**. The remarkably strong enhancement of second-hyperpolarizability of the inverse sandwiches with increasing size, **MIS-I** < **MIS-II** < **MIS-III** may be explained by the exceptional lowering of the transition energy for the marginal difference of the oscillator strength (eq 10). On the basis of this trend of cubic polarizability, the higher-order **MIS** complexes may be designed to obtain much larger NLO responses. Thus, a new structure property correlation can be obtained in optimizing the second-hyperpolarizability. As can be seen from Figure 1, the substantially lower energy electronic transition of the inverse sandwiches involves the symmetric charge transfer leading to the significant depletion of electron density on the middle Be atoms and the accumulation of electron density on the terminal metal atoms.

The figure of merit of the chosen multidecker inverse sandwiches as third-order NLO materials can be judged appropriately by comparing with other molecular systems. As for example the second-hyperpolarizability (in 10^6 au) of linear polyacetylene [H-(HC═CH)$_n$-H][49] and polyyne [H-(C≡C)$_n$-H][55] chains obtained at B3LYP/POL and B3LYP/cc-pVDZ levels, respectively, increases with increasing chain length in the following order: 4.04, 9.08, and 17.91 for polyacetylenes and 1.76, 3.91, and 7.74 for polyynes for n = 6, 7 and 8, respectively. On the other hand, γ values (in 10^6 au) obtained for the investigated complexes **MIS-I**, **MIS-II**, and **MIS-III** (having less or same number of atoms other than H atoms compared to those of linear chains) shows much larger enhancement on increasing size, 1.18, 5.16, and 11.75. Again in comparison to the charge transfer Ruthenium complexes trans-[Ru(4,4′-C≡CC$_6$H$_4$C≡CC$_6$H$_4$NO$_2$)Cl(dppm)$_2$][56] ($\langle\gamma\rangle$ = 4.6 × 10^5 au) and trans-[Ru(4−C═CHC$_6$H$_4$C≡CC$_6$H$_4$NO2)Cl(dppm)$_2$]PF$_6$ ($\langle\gamma\rangle$ = 8.3 × 10^5 au), the present inverse sandwiches **MIS-II** and **MIS-III** have larger (by an order) magnitudes of $\langle\gamma\rangle$ (see Table 4). Previous theoretical results of $\langle\gamma\rangle$ (in 10^4 au) obtained for the diradical salts[23] show an increasing trend with increasing size of alkali metal atoms: 221.30 ($Li_2^{\bullet+}$ $TCNQ^{\bullet-}$), 313.68 ($Na_2^{\bullet+}$ $TCNQ^{\bullet-}$), and 790.56 ($K_2^{\bullet+}$ $TCNQ^{\bullet-}$), which is comparable to the increase of second-hyperpolarizability of the investigated multidecker inverse sandwich complexes. Thus the present investigation provides a new route to design high-performance NLO materials.

IV. CONCLUSION

The present study reveals that the thermal stability of multidecker inverse sandwich complexes of beryllium is greater than the conventional normal Be-sandwich complexes and predicts the possible existence of higher order MIS's that in the future may be extended to reach the limit of molecular wire. The chosen DFT functionals used in the present study ranging from pure to hybrid GGA to long-range corrected CAM-B3LYP

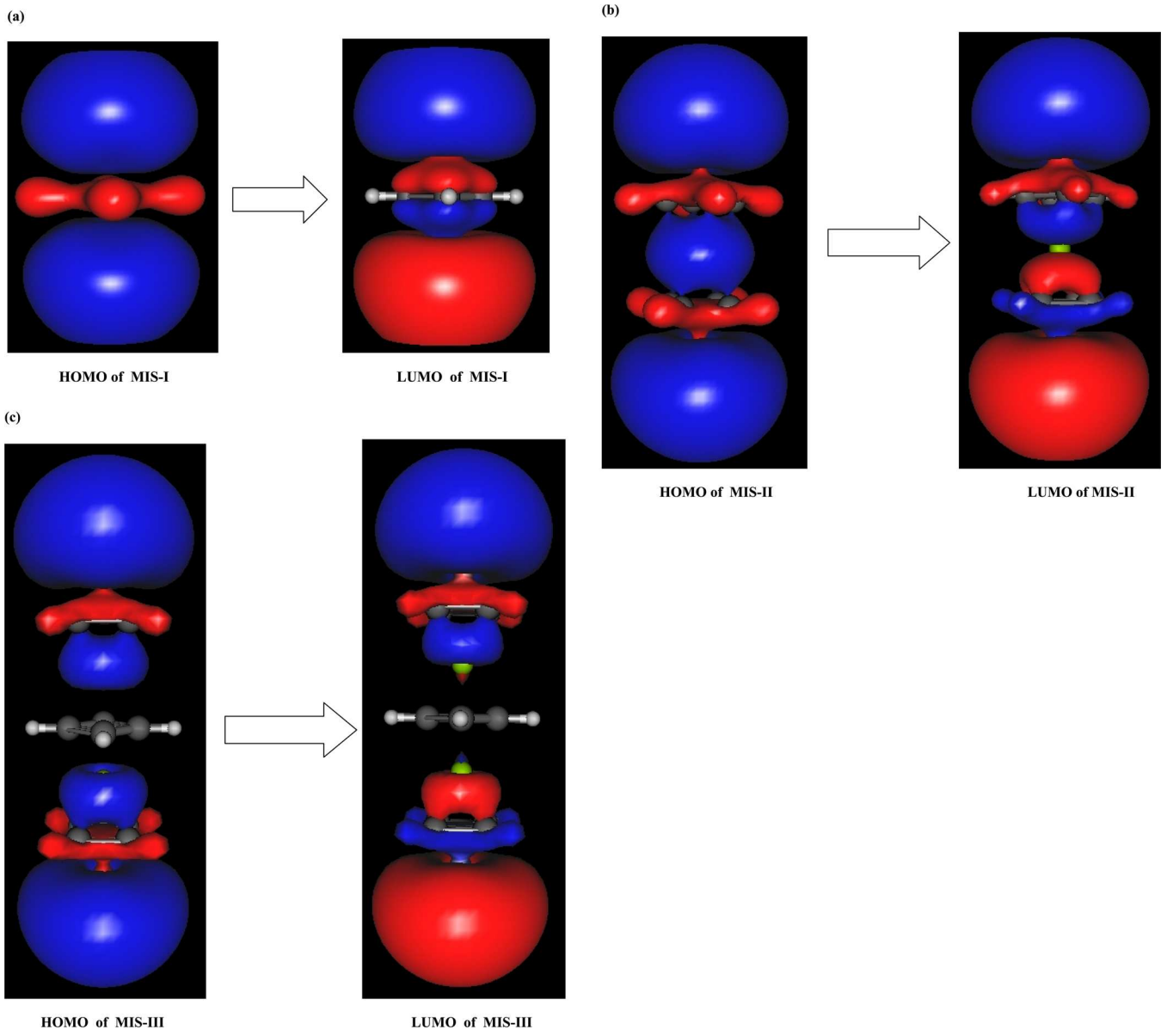

Figure 1. The three-dimensional surface plots of molecular orbitals involved in the major electronic transition of (a) **MIS-I**, (b) **MIS-II**, and (c) **MIS-III** complexes. All surfaces are drawn for the contour value of 0.01.

provide fairly consistent results of both polarizability and second-hyperpolarizability. The preferable choice of multidecker inverse sandwiches over the corresponding sandwich complexes as the potential NLO-phores is due to their appreciably large enhancement of second-hyperpolarizability on increase in the size. The evolution of the third-order response property of the chosen Be-complexes has been satisfactorily rationalized in terms of the spectroscopic properties relevant to the most intense electronic transition.

■ ASSOCIATED CONTENT

Supporting Information

Longitudinal component of polarizability and the average polarizability are given in Table S1. This material is available free of charge via the Internet at http://pubs.acs.org.

■ AUTHOR INFORMATION

Corresponding Author

*E-mail: nandi_pk@yahoo.co.in. Fax: +91 33 2668 2916.

Notes

The authors declare no competing financial interest.

■ ACKNOWLEDGMENTS

P.K.N. acknowledges the grant from UGC, Government of India under the Major Research Project (F. No. 42-339/2013 (SR) for carrying out this research work.

■ REFERENCES

(1) Kanis, D. R.; Ratner, M. A.; Marks, T. J. Design and Construction of Molecular Assemblies with Large Second-order Optical Nonlinearities. Quantum Chemical Aspects. *Chem. Rev.* **1994**, *94*, 195−242.

(2) Prasad, P. N.; Williams, D. J. *Introduction to Nonlinear Optical Effects in Molecules and Polymers*; Wiley-Interscience: New York, 1991.

(3) Mayers, F.; Marder, S. R.; Perry, J. W. Introduction to the Nonlinear Optical Properties of Organic Materials. In *Chemistry of Advanced Materials*; Interrante, L. V., Hampden-Smith, M. J., Eds.; Wiley-VCH: New York, 1998; pp 207−269.
(4) Nandi, P. K.; Panja, N.; Kar, T. Hyperpolarizabilities of Hetero-Cycle Based Chromophores: A Semi-Quantitative SOS Scheme. *Chem. Phys. Lett.* **2007**, *444*, 366−374.
(5) Nandi, P. K.; Panja, N.; Ghanty, T. K. Heterocycle-Based Isomeric Chromophores with Substantially Varying NLO Properties: A New Structure−Property Correlation Study. *J. Phys. Chem. A* **2008**, *112*, 4844−4852.
(6) Nandi, P. K.; Panja, N.; Ghanty, T. K.; Kar, T. Theoretical Study of the Effect of Structural Modifications on the Hyperpolarizabilities of Indigo Derivatives. *J. Phys. Chem. A* **2009**, *113*, 2623−2631.
(7) Panja, N.; Ghanty, T. K.; Nandi, P. K. A Sum-Over-State Scheme of Analysis of Hyperpolarizabilities and its Application to Spiroconjugated Molecular System. *Theor. Chem. Acc.* **2010**, *126*, 323−337.
(8) Hatua, K.; Nandi, P. K. Relationship Between Diffrent Order Polarizability and Ground State Dipole Moment. *J. Theor. Comput. Chem.* **2013**, *12*, 1250099.
(9) Bonness, S.; Fukui, H.; Yoneda, K.; Kishi, R.; Champagne, B.; Botek, E.; Nakano, M. Theoretical Investigation on the Second Hyperpolarizabilities of Open-Shell Singlet Systems by Spin-Unrestricted Density Functional Theory with Long-range Correction: Range Separating Parameter Dependence. *Chem. Phys. Lett.* **2010**, *493*, 195−199.
(10) Nakano, M.; Kubo, T.; Kamada, K.; Ohta, K.; Kishi, R.; Ohta, S.; Nakagawa, N.; Takahashi, H.; Furukawa, S.; Morita, Y.; et al. Second Hyperpolarizabilities of Polycyclic Aromatic Hydrocarbons Involving Phenalenyl Radical Units. *Chem. Phys. Lett.* **2006**, *418*, 142−147.
(11) Nakano, M.; Nagai, H.; Fukui, H.; Yoneda, K.; Kishi, R.; Takahashi, H.; Shimizu, A.; Kubo, T.; Kamada, K.; Ohta, K.; et al. Theoretical Study of Third-Order Nonlinear Optical Properties in Square Nanographenes with Open-Shell Singlet Ground States. *Chem. Phys. Lett.* **2008**, *467*, 120−125.
(12) Soldán, P.; Lee, E. P. F.; Wright, T. G. Static Dipole Polarizabilities (α) and Static Second Hyperpolarizabilities (γ) of the Rare Gas Atoms (He−Rn). *Phys. Chem. Chem. Phys.* **2001**, *3*, 4661−4666.
(13) Avramopoulos, A.; Reis, H.; Li, J.; Papadopoulos, M. G. The Dipole Moment, Polarizabilities, and First Hyperpolarizabilities of HArF. A Computational and Comparative Study. *J. Am. Chem. Soc.* **2004**, *126*, 6179−6184.
(14) Liu, Z. B.; Li, Z. R.; Zuo, M. H.; Li, Q. Z.; Ma, F.; Li, Z. J.; Chen, G. H.; Sun, C. C. Rare Gas Atomic Number Dependence of the Hyperpolarizability for Rare Gas Inserted Fluorohydrides, HRgF (Rg = He, Ar, and Kr). *J. Chem. Phys.* **2009**, *131*, 044308−(1−6).
(15) Avramopoulos, A.; Serrano, A. L.; Li, J.; Papadopoulos, M. G. On the Electronic Structure of H−Ng−Ng−F (Ng = Ar, Kr, Xe) and the Nonlinear Optical Properties of HXe_2F. *J. Chem. Theory Comput.* **2010**, *6*, 3365−3372.
(16) Xu, H. L.; Sun, S. L.; Muhammad, S.; Su, Z. M. Three-Propeller-Blade-Shaped Electride: Remarkable Alkali-Metal-Doped Effect on the First Hyperpolarizability. *Theor. Chem. Acc.* **2011**, *128*, 241−248.
(17) Ichimura, A. S.; Dye, J. L.; Camblor, M. A.; Villaescusa, L. A. Toward Inorganic Electrides. *J. Am. Chem. Soc.* **2002**, *124*, 1170−1171.
(18) Muhammad, S.; Xu, H. L.; Liao, Y.; Kan, Y. H.; Su, Z. M. Quantum Mechanical Design and Structure of the Li@$B_{10}H_{14}$ Basket with a Remarkably Enhanced Electro-Optical Response. *J. Am. Chem. Soc.* **2009**, *131*, 11833−11840.
(19) Dye, J. L. Electrons as Anions. *Science* **2003**, *301*, 607−608.
(20) Chen, W.; Li, Z. R.; Wu, D.; Li, Y.; Sun, C. C.; Gu, F. L. The Structure and the Large Nonlinear Optical Properties of Li@Calix[4]pyrrole. *J. Am. Chem. Soc.* **2005**, *127*, 10977−10981.
(21) Xu, H. L.; Li, Z. R.; Wu, D.; Wang, B. Q.; Li, Y.; Gu, F. L.; Aoki, Y. Structures and Large NLO Responses of New Electrides: Li-Doped Fluorocarbon Chain. *J. Am. Chem. Soc.* **2007**, *129*, 2967−2970.
(22) Champagne, B.; Spassova, M .; Jardin, J.; Kartin, B. Periodic Density Functional Theory Calculations for Na-Doped Quasi-One-Dimensional Polyacetylene Chains. *J. Phys. Chem. C* **2008**, *112*, 9493−9500.
(23) Li, Z. J.; Wang, F. F.; Li, Z. R.; Xu, H. L.; Huang, X. R.; Wu, D.; Chen, W.; Yu, G. T.; Gu, F. L.; Aoki, Y. Large Static First and Second Hyperpolarizabilities Dominated by Excess Electron Transition for Radical Ion Pair Salts M_2^{+}·+TCNQ·− (M = Li, Na, K). *Phys. Chem. Chem. Phys.* **2009**, *11*, 402−408.
(24) Kang, L. Z.; Inerbaev, T.; Kirtman, B.; Gu, F. L. Alkali Metal Doping Effect on Static First Hyperpolarizabilities of PMI Chains. *Theor. Chem. Acc.* **2011**, *130*, 727−737.
(25) Xu, H. L.; Zhang, C. C.; Sun, S. L.; Su, Z. M. Assembly of Sandwich-like Supermolecules Li Salts CpLi-C_{60}: Structure, Stabilities, and Nonlinear Optical Properties. *Organometallics* **2012**, *32*, 4409−4414.
(26) Xu, H. L.; Zhong, R. L.; Sun, S. L.; Su, Z. M. Widening or Lengthing? Enhancing First Hyperpolarizability of Tubiform Multi-lithium Salts. *J. Phys. Chem. C* **2011**, *115*, 16340−16346.
(27) Zhong, R. L.; Xu, H. L.; Sun, S. L.; Qiu, Y. Q.; Su, Z. M. The Excess Electron in a Boron Nitride Nanotube: Pyrimidal NBO Charge Distribution and Remarkable First Hyperpolarizability. *Chem.—Eur. J.* **2012**, *18*, 11350−11355.
(28) Hatua, K.; Nandi, P. K. Theoretical Study of Electronic Structure and Third-Order Optical Properties of Beryllium−Hydrocarbon Complexes. *Comput. Theor. Chem.* **2012**, *996*, 82−90.
(29) Mahadevi, S. A.; Sastry, G. N. A Theoretical Study on Interaction of Cyclopentadienyl Ligand with Alkali and Alkaline Earth Metals. *J. Phys. Chem. B* **2011**, *115*, 703−710.
(30) Cerpa, E.; Tenorio, F. J.; Contreras, M.; Villanueva, M.; Beltran, H. I.; Heine, T.; Donald, K. J.; Merino, G. Pentadienyl Complexes of Alkali Metals: Structure and Bonding. *Organometallics* **2008**, *27*, 827−833.
(31) Dinnebier, R. E.; Behrenns, U.; Olbrich, F. Solid State Structures of Cyclopentadienyllithium, Sodium, and -Potassium. Determination by High-Resolution Powder Diffraction. *Organometallics* **1997**, *16*, 3855−3858.
(32) Wilans, M. J.; Schurko, R. W. A Solid-State NMR and Ab Initio Study of Sodium Metallocenes. *J. Phys. Chem. B* **2003**, *107*, 5144−5161.
(33) Widdifield, C. M.; Schurko, R. W. A Solid-State 39K and 13C NMR Study of Polymeric Potassium Metallocenes. *J. Phys. Chem. A* **2005**, *109*, 6865−6876.
(34) Rayon, V. M.; Frenking, G. Structures, Bond Energies, Heats of Formation, and Quantitative Bonding Analysis of Main-Group Metallocenes [$E(Cp)_2$] (E = Be−Ba, Zn, Si−Pb) and [E(Cp)] (E = Li−Cs, B−Tl). *Chem.—Eur. J.* **2002**, *20*, 4693−4707.
(35) Velazquez, A.; Fernandez, I.; Frenking, G.; Merino, G. Multimetallocenes. A Theoretical Study. *Organometallics* **2007**, *26*, 4731−4736.
(36) Ning, H.; Hong-B, X.; Yi, H. D. One-electron Metal-metal Bond Stabilized in Dinuclear Metallocenes: Theoretical Predication of DBe-Li-Cp (D = C_5H_5 or C_5Me_5). *J. Phys. Chem. A* **2008**, *112*, 12463−12468.
(37) He, N.; Xie, H.-B.; Ding, Y. Can Donor-acceptor Bonded Dinuclear Metallocenes Exist? A Computational Study on the Stability of CpM′-MCp (M′ = B, Al, Ga, In, Tl; M = Li, Na, K) and its Isomers. *Organometallics* **2007**, *26*, 6839−6843.
(38) Xie, Y.; Schaefer, H. F., III; Jemmis, E. D. Characteristics of Novel Sandwiched Beryllium, Magnesium and Calcium Dimers: $C_5H_5BeBeC_5H_5$, $C_5H_5MgMgC_5H_5$, $C_5H_5CaCaC_5H_5$. *Chem. Phys. Lett.* **2005**, *402*, 414−421.
(39) Buchin, B.; Gemel, C.; Cadenbach, T.; Schmid, R.; Fischer, R. A. The $[Ga_2(C_5Me_5)]^{+}$ ion: Bipyramidal Double-cone Structure and Weakly Coordinated, Monovalent Ga^{+}. *Angew. Chem., Int. Ed.* **2006**, *45*, 1074−1076.
(40) Fernandez, I.; Cepra, E.; Frenking, G.; Merino, G. Structure and Bonding of $[E\text{-}Cp\text{-}E']^{+}$ Complexes (E and E′= B-Tl; Cp = Cyclopentadienyl). *Organometallics* **2008**, *27*, 1106−1111.
(41) Liu, N.-N.; Xu, J.; Ding, Y.-H. Inverse Sandwich Complexes Based on Low-valent Group 13 Elements and Cyclobutadiene: A Theoretical Investigation on E-C_4H_4-E (E= Al, Ga, In, Tl). *Int. J. Quantum Chem.* **2012**, *113*, 1018−1025.

(42) Becke, A. D. Density-Functional Exchange-Energy Approximation with Correct Asymptotic-Behavior. *Phys. Rev. A* **1988**, *38*, 3098−3100.
(43) Lee, C.; Yang, W.; Parr, R. G. Development of the Colle-Salvetti Correlation-Energy Formula into a Functional of the Electron Density. *Phys. Rev. B* **1988**, *37*, 785−89.
(44) Becke, A. D. Density-Functional Thermochemistry. III. The Role of Exact Exchange. *J. Chem. Phys.* **1993**, *98*, 5648−5652.
(45) Frisch, M. J.; Trucks, G. W.; Schlegel, H. B.; Scuseria, G. E.; Robb, M. A.; Cheeseman, J. R.; Scalmani, G.; Barone, V.; Mennucci, B.; Petersson, G. A.; Nakatsuji, H.; Caricato, M.; Li, X.; Hratchian, H. P.; Izmaylov, A. F.; Bloino, J.; Zheng, G.; Sonnenberg, J. L.; Hada, M.; Ehara, M.; Toyota, K.; Fukuda, R.; Hasegawa, J.; Ishida, M.; Nakajima, T.; Honda, Y.; Kitao, O.; Nakai, H.; Vreven, T.; Montgomery, J. A., Jr.; Peralta, P. E.; Ogliaro, F.; Bearpark, M.; Heyd, J. J.; Brothers, E.; Kudin, K. N.; Staroverov, V. N.; Kobayashi, R.; Normand, J.; Raghavachari, K.; Rendell, A.; Burant, J. C.; Iyengar, S. S.; Tomasi, J.; Cossi, M.; Rega, N.; Millam, N. J.; Klene, M.; Knox, J. E.; Cross, J. B.; Bakken, V.; Adamo, C.; Jaramillo, J.; Gomperts, R.; Stratmann, R. E.; Yazyev, O.; Austin, A. J.; Cammi, R.; Pomelli, C.; Ochterski, J. W.; Martin, R. L.; Morokuma, K.; Zakrzewski, V. G.; Voth, G. A.; Salvador, P.; Dannenberg, J. J.; Dapprich, S.; Daniels, A. D.; Farkas, Ö.; Ortiz, J. V.; Cioslowski, J.; Fox, D. J. *Gaussian 09*, Revision A.02; Gaussian, Inc.: Wallingford, CT, 2009.
(46) Yanai, T.; Tew, D.; Handy, N. A New Hybrid Exchange-Correlation Functional using the Coulomb-Attenuating Method (CAM-B3LYP). *Chem. Phys. Lett.* **2004**, *393*, 51−57.
(47) Grimme, S. Semiempirical Hybrid Density Functional with Perturbative Second-Order Correlation. *J. Chem. Phys.* **2006**, *124*, 034108−(1−16).
(48) Zhao, Y.; Truhlar, D. G. The M06 Suite of Density Functionals for Main Group Thermochemistry, Thermochemical Kinetics, Noncovalent Interactions, Excited States, and Transition Elements: Two New Functionals and Systematic Testing of Four M06-Class Functionals and 12 other Functionals. *Theor. Chem. Acc.* **2008**, *120*, 215−41.
(49) Limacher, P. A.; Mikkelsen, K. V.; Lüthi, H. P. On the Accurate Calculation of Polarizabilities and Second Hyperpolarizabilities of Polyacetylene Oligomer Chains using the CAM-B3LYP Density Functional. *J. Chem. Phys.* **2009**, *130*, 194114−(1−7).
(50) Alparone, A. Comparative Study of CCSD(T) and DFT Methods: Electronic (Hyper)polarizabilities of Glycine. *Chem. Phys. Lett.* **2011**, *514*, 21−25.
(51) Dunning, T. H. Gaussian Basis Sets for Use in Correlated Molecular Calculations. I. The Atoms Boron Through Neon and Hydrogen. *J. Chem. Phys.* **1989**, *90*, 1007−1023.
(52) Woon, D. E.; Dunning, T. H., Jr. Gaussian-Basis Sets for Use in Correlated Molecular Calculations. 3. The Atoms Aluminum through Argon. *J. Chem. Phys.* **1993**, *98*, 1358−71.
(53) Peach, M. J. G.; Helgaker, T.; Salek, P.; Keal, T. W.; Lutnæs, O. B.; Tozer, D. J.; Handy, N. C. Assessment of a Coulomb-Attenuated Exchange−Correlation Energy Functional. *Phys. Chem. Chem. Phys.* **2006**, *8*, 558−562.
(54) Wong, B. M.; Hsieh, T. H. Optoelectronic and Excitonic Properties of Oligoacenes: Substantial Improvements from Range-Separated Time-Dependent Density Functional Theory. *J. Chem. Theor. Comput.* **2010**, *6*, 3704−3712.
(55) Song, J.-W.; Watson, M. A.; Sekino, H.; Hirao, K. Nonlinear Optical Property Calculations of Polyynes with Long-Range Corrected Hybrid Exchange-Correlation Functional. *J. Chem. Phys.* **2008**, *129*, 024117−(1−8).
(56) Hurst, S. K.; Cifuentes, M. P.; Morrall, J. P. L.; Lucas, N. T.; Whittall, I. R.; Humphrey, M. G.; Asselberghs, I.; Persoons, A.; Samoc, M.; Luther-Davies, B.; et al. Organometallic Complexes for Nonlinear Optics. 22.[1] Quadratic and Cubic Hyperpolarizabilities of *trans*-Bis(bidentate phosphine)ruthenium ó-Arylvinylidene and ó-Arylalkynyl Complexes. *Organometallics* **2001**, *20*, 4664−4675.